REFERENCE

[1] Reston Condit and Dr. Douglas W. Jones, *Stepping Motors Fundamentals*, - AN907 - Microchip Technology, 2004.

[2] Hazem I. Al, *Robust QFT Controller Design for Positioning a Permanent Magnet Stepper Motors*, International Journal of Computer and Electrical Engineering, Vol. 1, No. 1, April 2009.

[3] Marc Bodson, John N. Chiasson, Robert T.Novotnak and Ronald B. Rekowski, *High Performance Nonlinear Feedback Control of a permanent Magnet Stepper Motor*, IEEE Transactions on Control Systems technology, VOL. 1, NO. 1, pp5-14, March1993.

[4] Tunable laser, *http://en.wikipedia.org/wiki/Tunable_laser.*

[5] Tunable laser*, http://www.opticsjournal.com/tutorial.htm.*

[6] Laser Beam, *http://web.princeton.edu/sites/ehs/laserguide/index.htm*.

[7] Laser types, *http://en.wikipedia.org/wiki/List_of_laser_types.*

[8] Laser property, *http://www.worldoflasers.com/laserproperties.htm.*

[9] Nandha Kumar Thulasiraman, Haider A.F. Mohamed and YeapSoo Cheng, *A reconfigurable wireless stepper motor controller based on FPGA implementation*, IEEE Symposium on Industrial Electronics and Applications, October 2010.

[10] Zhaojin Wen, Weihai Chen, ZhiyueXu and Jianhua Wang, *Analysis of Two-Phase Stepper Motor Driver Based on FPGA*, IEEE International Conference on Industrial Informatics, 2006.

[11] Wang Bangji, Liu Qingxiang, Zhou Lei, Zhang Yanrong, Li Xiangqiang and Zhang Jianqiong, *Velocity Profile Algorithm Realization on FPGA for Stepper Motor Controller*, IEEE International Conference, August 2011.

[12] Moussa Bendjedia, Youcef Ait-Amirat, Bernard Walther, and Alain Berthon, *Position Control of a Sensorless Stepper*, IEEE Transactions on Power Electronics, VOL. 27, N0. 2, February 2012.

[13] Kenneth Wang-Hay Tsui, Norbert Chow Cheung and Kadett Chi-Wah Yuen, *Novel Modeling and Damping Technique for Hybrid Stepper Motor*, IEEE Transactions on Industrial Electronics, VOL. 56, NO. 1, pp 202-211, January 2009.

[14] P. Acarnley, *Stepping Motors - A Guide to Modern Theory and Practice*, 4th ed. London, U.K.: The Institution of Engineering and Technology, 2002. ISBN (10 digit) 0 85296 417 X.

[15] Alexandru Morar, *Stepper motor modeling for the dynamic simulation*, Researchgate, VOL 44, November 2003.

[16] M. S. M. Elksasy and Hesham H.Gad, *A new Technique for Controlling Hybrid Stepper Motor through Modified PID Controller*, EBSCO HOST International Journal of Electrical& Computer Sciences, VOL 10, No. 2, pp29-39, April 2010.

[17] Wonhee Kim, Donghoon Shin, and Chung Choo Chung, *Microstepping Using a Disturbance Observer and a Variable Structure Controller for Permanent Magnet Stepper Motors*, IEEE Transactions on industrial Electronic, 2012.

[18] Anish NK, Deepak Krishnan, S. Moorthi and M.P. Selvan, *FPGA Based Microstepping Scheme for Stepper Motor in Space-Based Solar Power Systems*, IEEE International Conference on Industrial and Information Systems (ICIIS), pp 1-5, August 2012.

[19] Reston Condit, *Stepper Motor Control Using the PIC16F684*, -AN906 - Microchip Technology, 2004.

[20] Microsteping, *http://www.stepperworld.com/Tutorials/pgMicrostepping.htm.*

[21] Kim Otten, *USB Embedded Host Stack*, -AN1140 - Microchip Technology, 2008.

[22] Slave microcontroller, *http://ww1.microchip.com/downloads/en/DeviceDoc/70135G.pdf,* dsPIC30F4011 datasheet.

[23] Motor Driver, *www.allegromicro.com/~/media/Files/Datasheets/A3995-Datasheet.ashx, A3995 datasheet,* A3995 datasheet.

[24] David L.jones, *PCB Design Tutorial*, 2004.

[25] Buck converter, *http://www.ti.com/product/tps5450,* TPS5450 Datasheet.

APPENDIX A: VOLTAGE CONVERTER DESIGN

Converter requirement:

$$\text{Maximum input voltage}\left(V_{in(\max)}\right) = 12.5V$$
$$\text{Minimum input voltage}\left(V_{in(\min)}\right) = 11.5V$$
$$\text{Output voltage}(V_{out}) = 5\text{V}$$
$$\text{Output ripple}\left(V_{pp(\max)}\right) = 0.5V$$
$$\text{Output Current}\left(I_{out}\right) = 1.2A$$

The basic design is done by SwitcherPro software depending on the basic requirement. Figure A.1 shows the schematic of the software design.

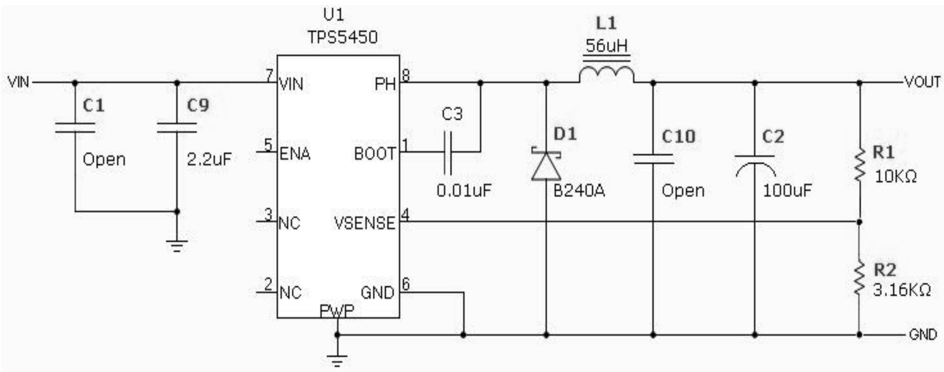

Figure A.1: Basic schematic get from the software

C1 and C9 capacitors are replaced with 220uF capacitors. The total system cost is reduced due to this replacement. Also, the input ripple is reduced, because the capacitor has less ESR and high capacitance. The input voltage ripple is calculated as follows.

$$\Delta V_{in} = \frac{\left(I_{OUT} \times 0.25\right) + \left(I_{OUT} \times ESR_{in(\max)}\right)}{C_{BULK} \times F_{SW}}$$

ΔV_{in} = Voltage ripple C_{BULK} = Input capacitance F_{SW} = Switching frequency

$ESR_{\max}$ = Maximum ESR of input capcitor

$$\Delta Vin = \frac{\left(1.2 \times 0.25\right) + (1.2 \times 900m\Omega)}{220\mu \times 500k}$$

$$= 0.0125V$$

$$V_{pk-pk} = 2\Delta V_{in}$$

$$= 0.025V$$

The voltage ripple is lesser than the required level, so this capacitor is suitable for this design. This capacitor can tolerate up to 25V, therefore, it can withstand the input voltage.

Inductor (L1) replaced with the 68µH. The inductor can tolerate up to 1.5A. Also, it reduces the current ripple in the output side and it eliminates the spikes in the output side. The RMS current and the maximum current are calculated as follows.

$$I_{L(RMS)} = \sqrt{\left(I_{out(\max)}\right)^2 + \frac{1}{12}\left(\frac{V_{out}\left(V_{in(\max)} - V_{OUT}\right)}{V_{In(MAX)}L_{OUT}F_{SW(MIN)}}\right)^2}$$

$$= \sqrt{(1.2)^2 + \frac{1}{12}\left(\frac{5\times(12.5-5)}{12.5\times 68\mu\times 500k}\right)^2}$$

$$= 1.44A$$

$$I_{L(PK)} = I_{OUT(MAX)} + \left(\frac{V_{OUT}\left(V_{IN(MAX)} - V_{OUT}\right)}{1.6V_{IN(MAX)}L_{OUT}F_{SW(MIN)}}\right)$$

$$= 1.2 + \left(\frac{5\times(12.5-5))}{1.6\times 12.5\times 68\mu\times 500k}\right)$$

$$= 1.255A$$

$I_{L(RMS)}$ = RMS current through the inductor

$I_{L(pk)}$ = Peck current through the inductor

L_{OUT} = Output inductance

$I_{L(RMS)}$ is lesser than the inductor maximum RMS current (1.5A). Also, $I_{L(PK)}$ is lesser than the saturation current of the inductor (1.4A). The calculation is done at maximum current. Therefore, this inductor is suitable for the design.

C2 capacitor is replaced with 330µF, because the output filtering is increased and the cost wise both are same. The cutoff frequency for output filleting can be calculated as follow. The maximum rated voltage is 6.3V; therefore it can tolerate the output voltage (5V).

$$F_{LC} = \sqrt{\left(\frac{85}{3357 L_{out} C_{OUT}}\right)}$$

$$= 1062.24 Hz$$

F_{LC} = Output filter cut off frequency

C_{OUT} = Output capacitor capacitance

F_{LC} is very lesser than the switching frequency (500kHz). Therefore, this capacitor and inductor value can produce a good filtering on the output side. The maximum allowable output capacitor ESR is calculated as follows.

$$ESR_{MAX} = \left(\frac{85 \times V_{OUT}}{2\pi C_{OUT} F_{LC}^{\;2}}\right)$$

$$= 182 m\Omega$$

ESR_{MAX} = Output capacitor maximum ESR

ESR maximum is greater than the C2 capacitor ESR (50mΩ). Therefore, it can be used for this application. Output voltage ripple for the selected components can be calculated as follows.

$$V_{PP(MAX)} = \frac{ESR \times V_{OUT}\left(V_{in(MAX)} - V_{OUT}\right)}{N_C V_{IN(MAX)} L_{OUT} F_{SW}}$$

$$= \frac{50 m\Omega \times 5 \times (12.5 - 5)}{1 \times 12.5 \times 68\mu \times 500k}$$

$$= 0.0044 V$$

ESR = ESR of the selected capacitor

$V_{pk\text{-}pk}$ is lesser than the required level (0.5V). Therefore, it satisfies the requirement. The component which was selected for this converter design can satisfy the specification.

APPENDIX B: MECHANICAL CALCULATION

Acceleration of the crystal:-

The maximum speed of the motor is 0.157rad/s. The time taken for the acceleration is 100µs. The speed of the motor and the load inertia are very low. Therefore, the motor can start the rotation immediately. The maximum acceleration time is equal to the minimum microsteps delay. The actual delay is more than this.

$$\text{Acceleration} = \frac{0.157}{100\mu}$$

$$= 1570.8 rad/s^2$$

Inertia of the crystal:-

Figure B.1 shows the load which is used for the application. The mass of the load is 0.3kg. The inertia for solid cuboids was calculated, but the load is not complete cuboids solid. Therefore, the actual inertia is lesser than the calculated value.

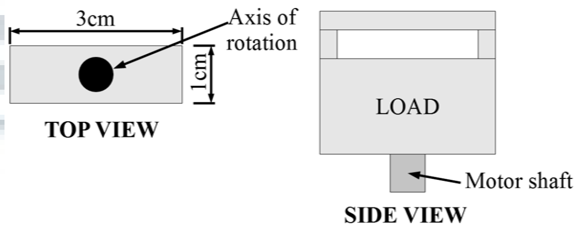

Figure B.1: Crystal mounts

$$\text{Load inertia} = \frac{m(w^2 + d^2)}{12}$$

$$= \frac{0.3(0.01^2 + 0.03^2)}{12}$$

$$= 2.5 \times 10^{-5} kgm^2$$

The crystal and the holder mass and the dimensions are lesser than this load. Therefore, the inertia of the crystal is lesser than the calculated value.

Starting torque:-

$$\text{Starting torque} = J\alpha$$

$$= 0.000025 \times 1570.8$$

$$= 0.0392 Nm$$

APPENDIX C: QEI MODULE DESCRIPTION

The incremental quadrature encoder generates the 3 pulse output. Those signals are QEA, QEB and index. The encoder generates the pulses depending on the angular position of the motor. The index signal is used to identify the reference (0^{th} position) of the motor. The index pulse generated position is considered as the reference point. Therefore, the index signal of the encoder is used to create the absolute position reading. There is a 90° phase shift between QEA and QEB signals. Figure C.1 shows the waveform of these signals. The encoder generates 10,000 pulses per revolution.

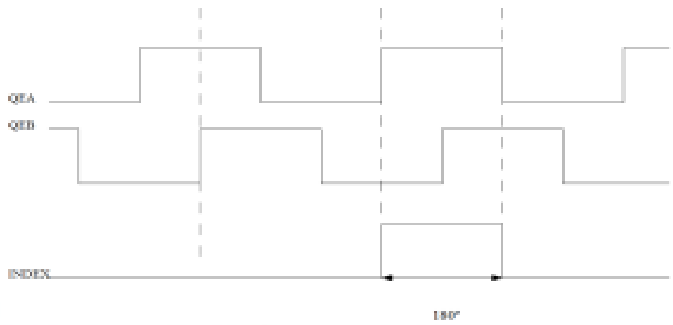

Figure C.1: Encoder pulse

The QEI module in the microcontroller is using these signals and counts the position. The QEI module increased and decreased the counter depending on the rotation direction. It uses the 16bit counter for the position counting. There are 2 different modes of counting in QEI module. Those are x2 and x4 mode. Figure C.2 shows the counter changing points in the waveform for each mode.

The QEI module can detect 4 positions within the one clock period in x4 mode. The encoder resolution is higher than the x2 mode. The QEI module can detect 40,000 positions in one revolution. Therefore, the encoder resolution is 0.009°, so x4 mode is selected for this design. The index pulse width covers the 2 encoder positions in x4 mode. The QEI module can select one position as the index position according to the configuration. We can select QEA and QEB logic value for the index position detection.

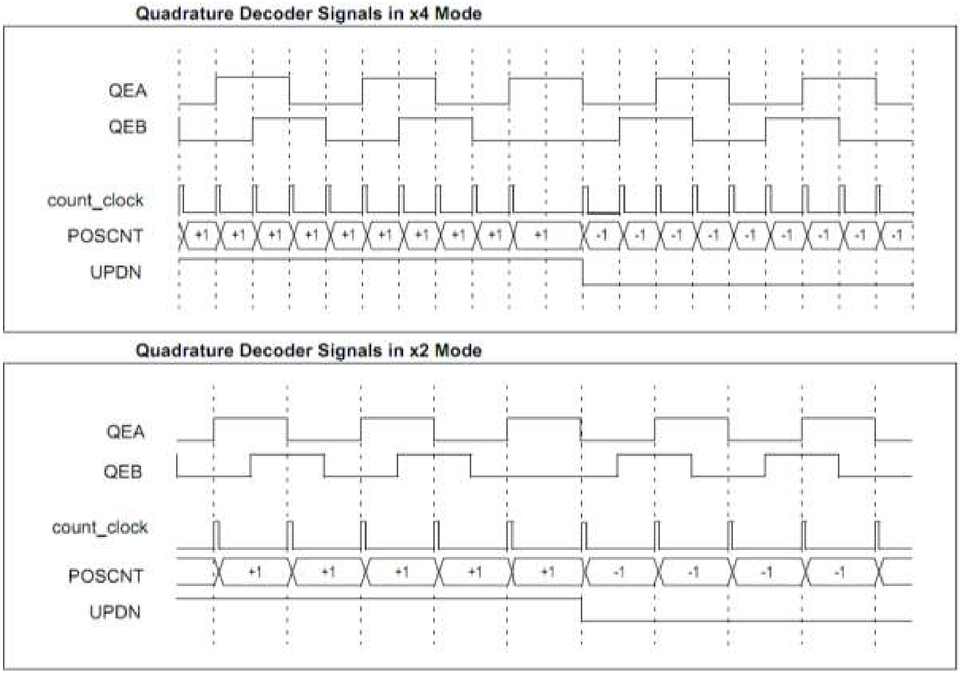

Figure C.2: Mode of counting

Example:-

The QEA and QEB should be logic 1 for detecting the index point. If the index pulse and another 2 signal are higher than only the index position will be detected.

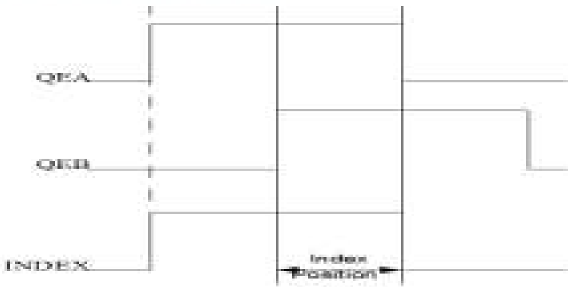

Figure C.3: Index detection

Table C.1: Encoder specification

Operation voltage	3.3 - 28V
Input current	100mA
Output format	incremental
Output type	Open collector
Pulses	10000 pulse per revolution
Index	One per revolution
Max Shaft speed	8000RPM
Bore size	5mm
Max Acceleration	1 x10^5rad/s^2
Starting torque	0.001Nm

<u>Digital filter</u>

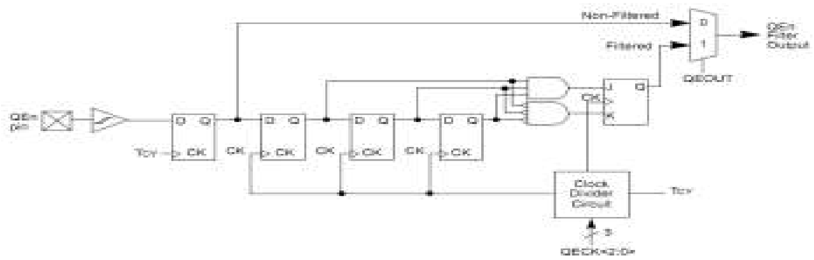

Figure C.4: Filter structure

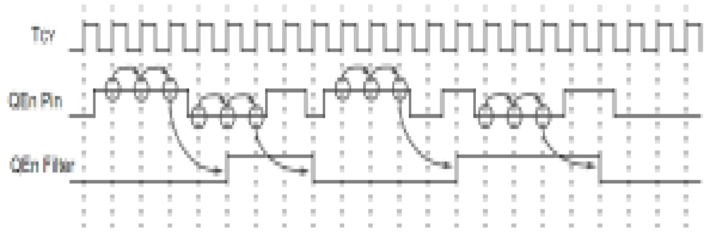

Figure C.5: Waveform of the filtering

Figure C.4 shows the filter structure. Figure C.5 shows the waveform of the filtered signal. T_{CY} clock is used to control the digital filtering. The period of the T_{cy} clock is 3.2µs. The state of the QE signal is decided after $4T_{cy}$ clock pulse. The filter creates the 12.8µs phase delay. It eliminates the short pulses generated by the noise. The pulses which have the period less than the 12.8µs are removed.

APPENDIX D: MOTOR SPECIFICATION

Motor specification:

- Maximum current per winding 0.21A.
- Resistance per winding 57.1Ω.
- The inductance of the winding is 32mH.

Maximum power loss per winding	=	$(I^2R) * 2$
	=	$(0.21^2) * 57.1 * 2$
	=	4.568W

The system is not battery powered. Therefore, this loss is not a problem. The motor case is made of metal, therefore the heat transfer to the environment quickly. The motor is not damaged due to the heat.

<u>Resonance vibration compared with the standard stepper motor</u>

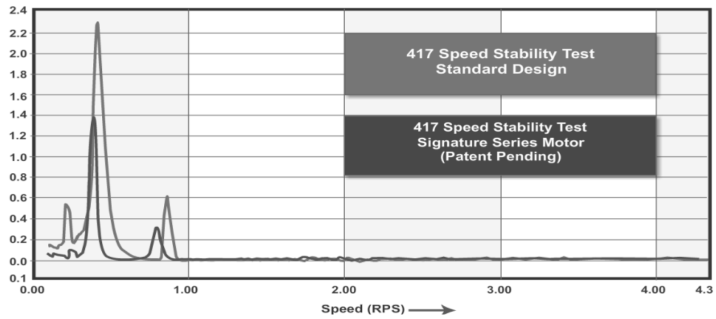

Figure D.1: Vibration comparison between the motor

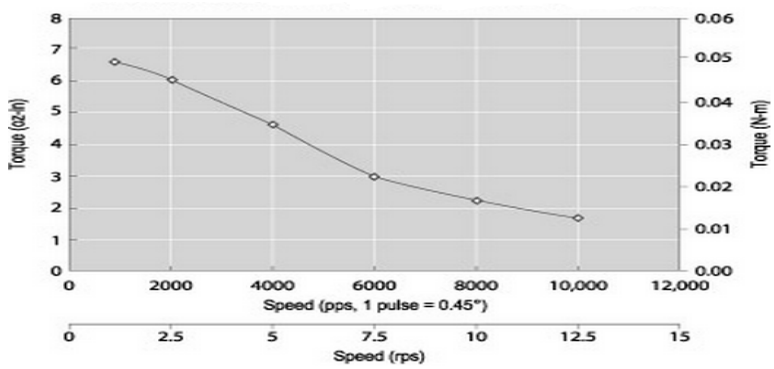

Figure D.2: Torque vs. speed